Monte Carlo simulation of polymer systems with topological constraints

Flikkema, Edwin

Chapter 4

Osmotic pressure of ring polymer solutions: A Monte Carlo study

E. Flikkema, G. ten Brinke
J. Chem. Phys **113**, 11393 (2000)

4.1 Introduction

Ring polymers have intriguing properties which has led to a continuous stream of publications over the last decades (e.g. Refs [10, 14, 16, 40–44]). Ring polymers differ from their linear counterparts by the topological constraints which force a ring polymer conformation to stay within the topological state of preparation. An unlimited number of different topological states (different knot structures and linkages) are possible. However, the synthesis of ring polymers requires extremely dilute solutions thereby strongly reducing the probability of catenate formation [45]. Moreover, if the synthesis takes place under good solvent conditions, knot formation is also strongly suppressed [14]. Therefore, in this chapter we will concentrate on unknotted and unconcatenated ring polymers. In a solution of these molecules, the topological constraint leads to an effective repulsion in addition to ordinary excluded vo-

lume effects. We will focus on this additional repulsion and consider a ring polymer solution under conditions corresponding to the θ-state of the corresponding linear chain. In such a system any interaction observed is solely due to the topological constraints.

4.2 Off-lattice model for ring polymer systems

In this chapter we will consider an off-lattice model for ring polymers. In this model a ring polymer molecule consists of point-like monomers ('beads') connected by bonds of a fixed length. The angle between consecutive bonds is not restricted in any way. This is sometimes referred to as the 'freely-jointed' model. Topological constraints are active: within a single ring as well as between rings. Although it is possible to include interaction potentials between monomers, we will focus on the case where there is only topological interaction. This corresponds to θ-conditions of the corresponding linear chains.

For comparison, we will also consider linear polymers with excluded volume interaction. Here the beads are spheres with a non-zero radius. These beads are not allowed to overlap. The beads are connected by bonds of a fixed length to form linear chains. Topological constraints are irrelevant here because the chains are not closed.

4.3 Monte Carlo algorithm

Monte Carlo simulation is used with a simulation algorithm that conserves the topological state. Beads are moved one at a time: the bead which is to be moved is chosen randomly from the beads in the system. The selected monomer $\vec{r}_i$ is rotated with a randomly chosen angle about the axis through the connected beads $\vec{r}_{i-1}$, $\vec{r}_{i+1}$ to its new position $\vec{r}_i'$. (See Fig. a in 4.1) To assure the conservation of the topological state, we imagine that the bead moves from its original position $\vec{r}_i$ to its new position $\vec{r}_i'$ along a straight line and require that during this motion the bonds connecting the moving bead to $\vec{r}_{i-1}$ and $\vec{r}_{i+1}$ do not cross any of the other bonds in the system. This amounts

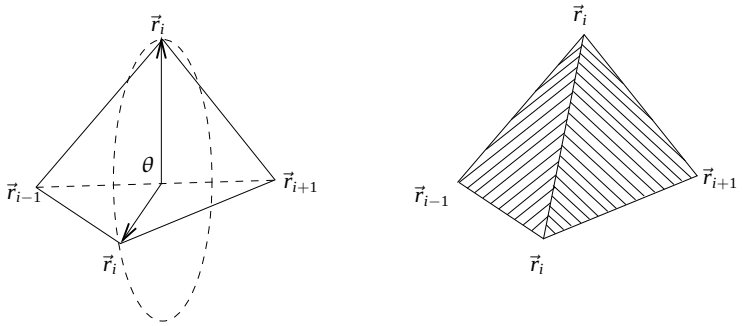

(a) (b)

Figure 4.1: (a) Illustration of Monte Carlo bead move; (b) non-crossing constraint consists of checking whether any bond in the system crosses any of the two triangles depicted.

to checking whether any bond in the system crosses the triangles indicated in Fig. b in 4.1. If the non-crossing constraint is violated, the move is rejected.

For the system of linear chains a similar rotation move is used, in combination with moves for the chain ends. The non-crossing constraint is not checked. Only excluded volume interaction is checked: moves are rejected if they lead to overlapping beads.

4.4 Pair of unknotted and unlinked rings

We start with the simplest of all ring polymer systems: a single ring polymer. As a test for the sampling algorithm rings of various sizes and knot-types have been simulated. We have verified that the knot-type does not change during the simulation. The averaged squared radius of gyration $\langle R_g^2 \rangle$ has been computed. The results are shown in fig. 4.2. It is apparent that the more complex knots (with more crossings) are smaller. One would expect that an unknotted ring is swollen compared to a ring without topological constraints, because the more compact knotted conformations are not included in the average size. However, in the simulations there is no significant deviation from the closed random walk result (derived in Appendix A), probably because N

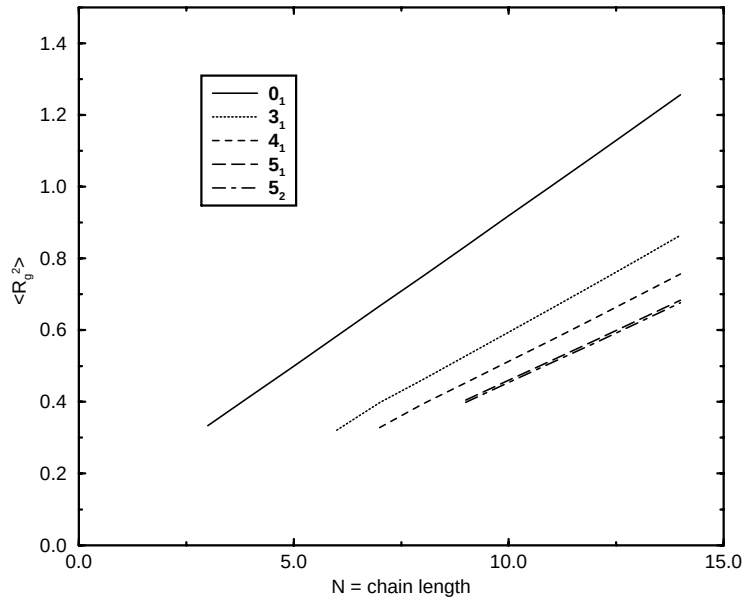

Figure 4.2: $\langle R_g^2 \rangle$ versus N for various knots.

is still relatively small in the simulations.

The next system we consider is a pair of ring polymers, focusing on the effect of the inter-molecular topological constraint. As explained in section 1.3 for a pair of unlinked rings the entropy of the system is reduced as we bring the rings closer together. To study this effect we have simulated two rings which were prepared in the unknotted and unconcatenated state. An umbrella potential was used to prevent the rings from moving too far away from each other. (Here a simple infinite well potential was used as an umbrella potential.) The topological interaction between the rings is derived from the histogram for the distance between the centers of mass. The histogram is proportional to the probability $P_0(r)$ of finding a pair of unknotted rings placed a distance r apart in the unconcatenated state. The proportionality constant is determined from the fact that $P_0(r) = 1$ for r sufficiently large. The result is shown in figure 4.3: $P_0(r)$ has been plotted versus r for various chain lengths $N = 8, 16, 24$. From this the second virial coefficient is

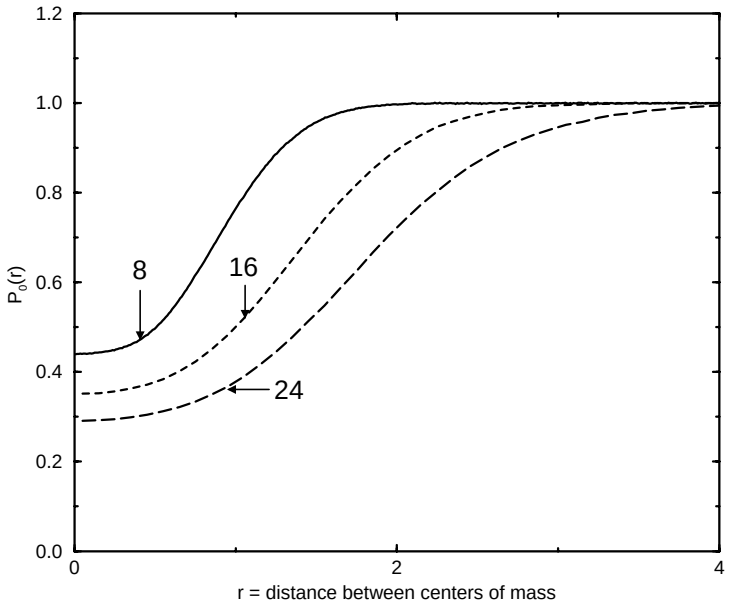

Figure 4.3: The probability $P_0(r)$ that two rings separated by a distance r are in the unentangled state.

calculated:

$$B = \frac{1}{2}\int (1 - P_0(r))4\pi r^2 dr \tag{4.1}$$

This approach leads to the values $B = 1.5$, 6.0 and 14.3 for $N = 8$, 16 and 24, respectively.

4.5 Wall Theorem

A very convenient method to determine the equation of state of a fluid by Monte Carlo simulations is based on the wall theorem [46–48], which states that the pressure of an isotropic fluid is given by

$$p = k_B T \rho(0) \tag{4.2}$$

where $\rho(0)$ is the density at the wall. This result can be easily derived from first principles. Our simulations deal with a simulation cell of dimensions

$L_x \times L_y \times L_z$ with hard walls. In the actual simulations $L_x = L_y = L_z = L$. These boundary conditions are represented by Heaviside step functions $\theta(x)$ in the following partition function for the case of N_p polymers, each consisting of N segments:

$$Q = \int \left[\prod_{i=1}^{N_p} \prod_{j=1}^{N} dx_i^{(j)} dy_i^{(j)} dz_i^{(j)} \right] \exp(-\beta U) \times \left[\prod_{i=1}^{N_p} \prod_{j=1}^{N} \theta(x_i^{(j)}) \theta(y_i^{(j)}) \theta(z_i^{(j)}) \theta(L_x - x_i^{(j)}) \theta(L_y - y_i^{(j)}) \theta(L_z - z_i^{(j)}) \right] \tag{4.3}$$

Here $x_i^{(j)}$ is the x-coordinate of the jth segment on the ith chain. U is the potential energy *including* the inter-segmental potentials that define the chain connectivity. The pressure is related to the derivative of Q with respect to the box size L_x in the following way

$$\frac{p}{k_B T} = \frac{1}{L_y L_z Q} \frac{\partial Q}{\partial L_x} \tag{4.4}$$

The derivative can be performed using the product rule and the fact that the derivative of the Heaviside step function is the Dirac delta function.
The density $\rho(0)$ at the wall is defined as

$$\rho(0) = \lim_{\epsilon \downarrow 0} \frac{1}{L_y L_z} \int_0^{L_y} dy \int_0^{L_z} dz \; \rho(\epsilon, y, z) \tag{4.5}$$

where $\rho(x, y, z)$ is defined as:

$$\rho(x,y,z) = \frac{1}{Q} \int \left[\prod_{i=1}^{N_p} \prod_{j=1}^{N} dx_i^{(j)} dy_i^{(j)} dz_i^{(j)} \right] \exp(-\beta U) \times \left[\prod_{i=1}^{N_p} \prod_{j=1}^{N} \theta(x_i^{(j)}) \theta(y_i^{(j)}) \theta(z_i^{(j)}) \theta(L_x - x_i^{(j)}) \theta(L_y - y_i^{(j)}) \theta(L_z - z_i^{(j)}) \right] \times \sum_{k=1}^{N_p} \sum_{l=1}^{N} \delta(x_k^{(l)} - x) \delta(y_k^{(l)} - y) \delta(z_k^{(l)} - z) \tag{4.6}$$

With a few manipulations one can show that (4.4) and (4.5) reduce to the same expression. The details can be found in appendix C.

4.6 Rings confined to a box

In this section we will consider ring polymers confined to a box as a model of ring polymers in solution at non-zero concentration. The inter-molecular topological constraint leads to an entropic repulsion resulting in an increase in the osmotic pressure.

We consider a box of size $L \times L \times L$ with hard walls. The use of hard walls allows us to calculate the osmotic pressure via the wall theorem (see section 4.5), which states that the pressure of a system of interacting particles (in units of kT) equals the density of the particles at the wall. In the past it has been successfully employed for linear chain molecules [49, 50]. Applied to our system, this implies that the osmotic pressure π of the ring polymer system is equal to the monomer density ρ_{wall} at a hard wall,

$$\frac{\pi}{kT} = \rho_{wall} \tag{4.7}$$

The density profile $\rho(x)$ has been calculated with walls situated at $x = 0$ and $x = L$. To this end, the box was divided into thin slices and the number of monomers in each slice counted and subsequently averaged over many snapshots. Figure 4.4 shows a characteristic density profile for 64 16-mers in an $L = 8$ box. The profile shows a strong decrease of the density near the walls due to the large amount of entropy-loss close to the wall. The same figure also shows the density profile for the corresponding phantom rings, i.e. without conservation of topology. The effect of the topology manifests itself clearly in an increased density at the wall.

The explanation is straightforward: phantom rings can avoid the reduction in conformational entropy near a hard wall by moving away from it. If topological constraints are present this happens to a lesser extent due to the topological repulsion between different rings. The density is varied by putting different numbers of rings in the box. Each simulation produces a density profile from which two numbers are extracted: the density at the wall ρ_{wall} and the bulk density ρ_{bulk}. ρ_{wall} is calculated by fitting the density profile near the wall to a line and extrapolating this line to $x = 0$ (or $x = L$ for the other wall). ρ_{bulk} corresponds to the height of the horizontal section of the density curve in the middle of the box. Hence, each simulation gives

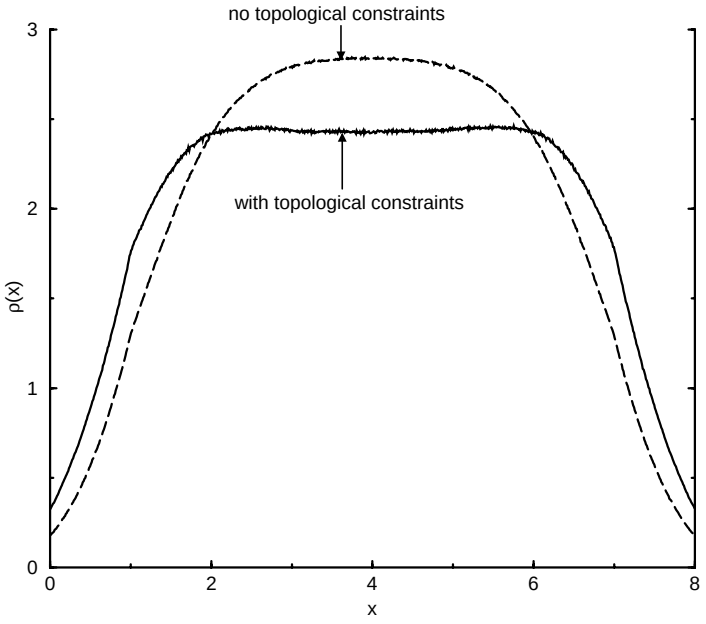

Figure 4.4: Density profile of a system consisting of 64 rings of size $N = 16$ in a box of $L = 8$. For comparison, the density profile for the same system but without topological constraints is also presented.

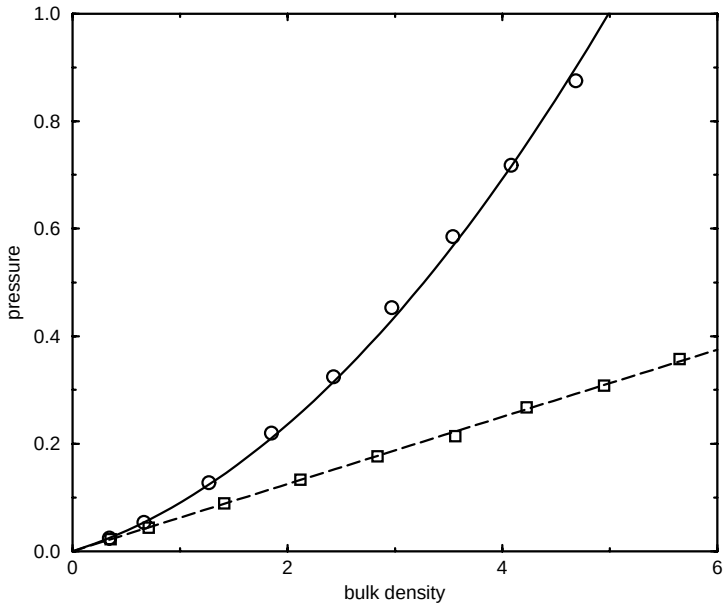

Figure 4.5: Pressure-density data (○), together with second virial approximation, Eq. (2) (solid line), for rings of size $N = 16$ in a box of size $L = 8$. For comparison the pressure-density data for the system without topological constraints is also given (□) together with the ideal gas law (dashed line).

a point in the pressure-density plane and all simulations combined give the equation of state.

The pressure-density curves have been calculated for rings of various sizes: $N = 8$, 16 and 24. Figure 4.5 shows the result for $N = 16$. The figure shows that the osmotic pressure of the system with topological constraints is considerably higher than for the phantom rings. In the latter case, the pressure-density curve is nothing but the ideal gas law with every ring polymer replaced by a single particle. The second virial coefficient B is related to the osmotic pressure in the following way:

$$\frac{\pi}{kT} = \rho_R + B\rho_R^2 + \cdots \tag{4.8}$$

where $\rho_R = \rho/N$ is the number of ring molecules per unit volume. Various least squares fits of the data to (4.8) have been performed, the results of which

Table 4.1: Second virial coefficient B, obtained by various methods.

	from $P(\rho)$			from $P_0(r)$
N	I	II	III	
8	1.509	1.525	1.613	1.475
16	5.555	6.118	7.083	5.978
24	14.240	14.852	16.720	14.311

have been summarized in table 4.1, together with the earlier results obtained via (4.1) The three columns labeled I, II and III correspond to different numbers of fitting parameters. In method I a second degree polynomial is used as a fit-function, all three coefficients being determined by fitting. In method II the constant term is fixed at the value zero, the coefficients of the linear and quadratic term being determined by fitting. In method III only the coefficient B of the quadratic term is determined by fitting, the coefficients of the constant and linear term being fixed to 0 and 1 respectively. The values for B are slightly different for the different methods. The discrepancy between the values of B derived from the pressure-density data and those derived from $P_0(r)$ is most likely due to the finite size of the box and the influence of the third virial coefficient. The theoretical analysis presented by Tanaka [51, 52] predicts a much stronger chain length dependence of B, which may at least be partly due to the relatively small chain lengths employed in our study.

To get an indication of the strength of the repulsion induced by the topological constraint, we consider next the linear counterpart with beads of finite size, a size tuned in such a way that the equations of state coincide. Figure 4.6 demonstrates that in the case of $N = 16$, a rather good fit is obtained for linear chains with beads of size $R = 0.113$. Deviations only start to occur at the highest densities. The same result is found for the other two chain lengths. Hence, as far as the osmotic pressure is concerned the ring polymer system under θ-conditions for the linear counterpart closely resembles a system of linear chains with an excluded volume effect corresponding to a bead size of $R = 0.113$. The topological constraints effectively amount to an additional

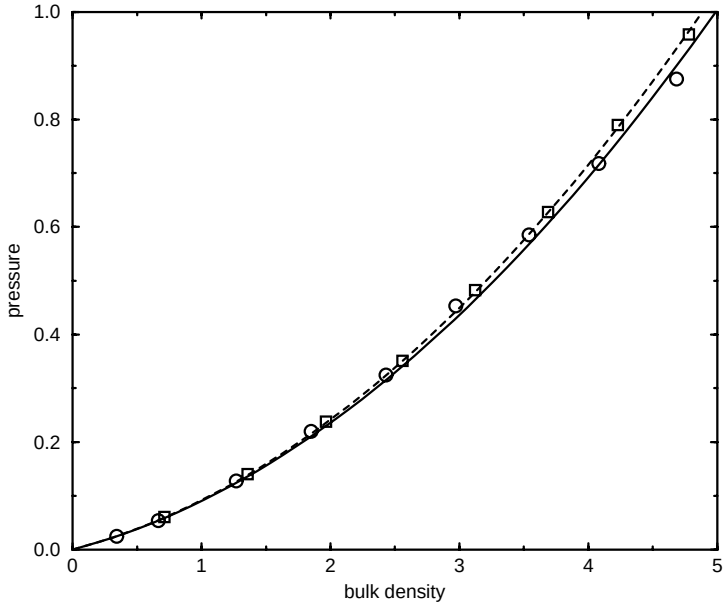

Figure 4.6: Pressure-density curve (○) of rings with topological constraints (but without excluded volume) compared to the pressure-density curve (□) of linear chains with excluded volume corresponding to beads of size $R = 0.113$.

excluded volume effect.

We can obtain a rough estimate for the temperature distance to the θ-temperature of the latter system. To this end we consider a freely-jointed linear chain model with beads of size $R = 0.5$ (in units of bond length). The excluded volume of such a system is approximately equal to

$$V_{excl} \approx \frac{2}{3}\pi(2R)^3(1-2\chi) \tag{4.9}$$

Here χ is the Flory-Huggins parameter, which usually is positive thereby reducing the excluded volume effect. An effective bead size of $R = 0.113$ would correspond in this picture to a value of $\chi = 0.494$. θ-conditions correspond to $\chi = 0.5$. In order to get some feeling for the corresponding temperature difference we use the temperature dependence for the χ-parameter of the polystyrene / cyclohexane system as given in Ref. [53],

$$\chi = \frac{64}{T} + 0.29 \tag{4.10}$$

For this particular parameterization $\chi = 0.494$ corresponds to $T = 313.7K$ and $\chi = 0.5$ to $T = 304.8K$. In this picture an effective excluded volume of $R = 0.113$ corresponds to a linear polymer system roughly $9K$ above its θ-conditions. In the case of polystyrene and cyclohexane, the literature value for the θ-temperature of ring polystyrene in cyclohexane is $301K$ compared to $308K$ for linear polystyrene [45]. Of course, the estimates presented should not be taken too seriously, however, the order of magnitude agreement is gratifying.

In summary, we have used the wall theorem to compute the osmotic pressure of ring polymers in solution. An off-lattice, topology conserving, Monte Carlo algorithm was used to simulate a freely jointed model with no other form of interaction than topological interaction. (This corresponds to θ-conditions for the corresponding linear chains.) The equation of state is determined and compared to linear chains with excluded volume interaction. It is demonstrated that a similar equation of state is found taking beads of size 0.113 in units of the bond length.